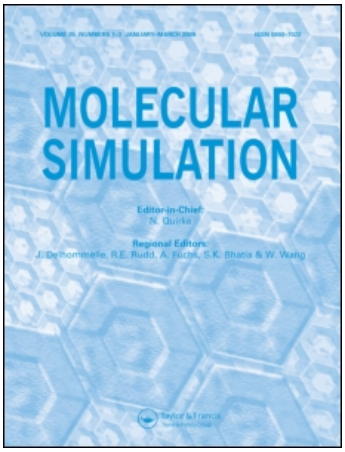

Molecular Simulation
Publication details, including instructions for authors and subscription information:
http://www.informaworld.com/smpp/title~content=t713644482

Monte Carlo-Self Consistent Field Study of the Symmetrical Models of Polyelectrolytes

P. N. Vorontsov-velyaminov[a]; A. P. Lyubartsev[a]
[a] Physics Faculty, St. Petersburg State University, Peterhoff, St. Petersburg, Russia

To cite this Article Vorontsov-velyaminov, P. N. and Lyubartsev, A. P.(1992) 'Monte Carlo-Self Consistent Field Study of the Symmetrical Models of Polyelectrolytes', Molecular Simulation, 9: 4, 285 — 306
To link to this Article: DOI: 10.1080/08927029208047434
URL: http://dx.doi.org/10.1080/08927029208047434

Molecular Simulation, 1992, Vol. 9(4), pp. 285–306
Reprints available directly from the publisher
Photocopying permitted by license only

MONTE CARLO–SELF CONSISTENT FIELD STUDY OF THE SYMMETRICAL MODELS OF POLYELECTROLYTES

P.N. VORONTSOV-VELYAMINOV and A.P. LYUBARTSEV

Physics Faculty, St. Petersburg State University, 198904, Peterhoff, St. Petersburg, Russia

(*Received March 1992, accepted March 1992*)

Time saving procedures unifying Monte Carlo and self consistent field approaches for the calculation of equilibrium potentials and density distributions of mobile ions around a polyion in a polyelectrolyte system are considered. In the final version of the method the region around the polyion is divided into two zones – internal and external; all the ions of the internal zone are accounted for explicitly in a Monte Carlo procedure, in the external zone the self consistent field approximation is applied with an exchange of ions between regions. Simulations are carried out for cylindrical and spherical polyions in solutions with mono- and divalent ions and their mixtures. The results are compared with Poisson–Boltzmann approximation and experimental data on intrinsic viscosity.

KEY WORDS: Polyelectrolytes, Monte Carlo, self consistent field, time saving algorithm

1 INTRODUCTION

Numerous macromolecules on being dissolved in water dissociate yielding a charged polyion surrounded by an atmosphere of small ions of the opposite sign (polyelectrolytes solution). In the presence of a salt the solution contains small ions of both signs. Electrostatic interactions strongly affect most of the properties of polyelectrolyte solutions: chain rigidity, conformation, electrochemical and thermal behavior, etc. The importance of polyelectrolyte solutions is particularly apparent in considering that the main biomacromolecules (above all DNA) are in fact strongly charged polyelectrolytes.

There exists considerable interest in the theorectical study of polyelectrolytes [1–10]. The main problem is to calculate the equilibrium electrostatic potential and charge density in the vicinity of the polyion in a fixed configuration. As a rule symmetrical models are considered with the polyion being represented by a uniformly charged sphere, cylinder or a plane. The basis of such an assumption is that the effective distance of the electrostatic forces is of the order of the Debye radius $r_D = 1/(8\pi l_B c)^{1/2}$ ($l_B = e^2/\varepsilon kT$ = Bjerrum length, c = ion strength). Inhomogeneities in charge distribution on the polyion surface having dimensions less than r_D are averaged and do not greatly effect the charge distribution of the mobile ions and equilibrium potential in the surrounding space. Such polyions as globular proteins, micelles or colloid particles are usually considered as uniformly charged spheres [3, 8, 9] and linear rigid polyions of the DNA-type – as infinite uniformly charged cylinders [1–5].

Even for such primitive models there exist no simple analytical solutions and the

use of integral equation approach yields to approximations with uncontrolled errors. The most popular approach is the self-consistent field approximation [3, 4] which yields the Poisson–Boltzmann (PB) equation for the equilibrium potential. As was shown earlier [2–4] this approximation is justified for cylindrical models of polyions in water solutions in the presence of monovalent ions (the error does not exceed 10% in the whole concentration range excluding (perhaps) only the highest concentrations). However in the case of divalent ions the PB eqaution is already inadequate, serious discrepancies appear between the PB approximation and other analytical approaches [3, 5] as well as several existing simulations [11, 12]. The applicability of more accurate analytical approaches (HNC-approximation [5, 8], modified Poisson–Boltzmann equation [13]) is also uncertain, moreover they could not be generalized to account for the specific charge distribution on the polyion.

In principle it is possible to obtain an accurate statistical-mechanical solution of the problem for the given model with the aid of computer experiments (Monte Carlo (MC) or molecular dynamics methods). However for systems with long range potentials where one should explicitly account for very great number of charges (such is the case for the polyelectrolyte solution) the computer time required can become very high.

Recently we have suggested several versions of a method unifying MC simulation with the self-consistent field approach (MC–SCF – [14–17]). This method allows to simulate directly only a fraction of all the ions and account for another (greater) part with the aid of the self consistent field. In Refs [14–16] there were suggested three versions of the method and some applications were demonstrated. However the simulation algorithms were not discussed in detail. In this paper we present a detailed summarized description of the algorithms (Sections 2 and 3), methodological data (Section 4) and new systematic results for the distribution of ions of various valencies around cylindrical (Section 5) and spherical (Section 6) polyions.

2 SIMPLEST VARIANTS OF MC–SCF METHOD

2.1 Random Walk of a Single Ion

Consider a polyion of the given conformation immersed in the electrolyte solution of volume V and creating the potential $\psi_0(x)$. Here and below we shall use dimensionless units: the potential ψ is related to the conventional potential ϕ by: $\psi = e\phi/kT$ (at room temperature $T = 300\,\mathrm{K}$ the value $\psi = 1$ corresponds to $\phi = 25\,\mathrm{mV}$); all distances are expressed in units of Bjerrum length l_B; density distributions are normalized on unit in the whole volume. Let s species of ions be present in solution, N_α being the ion number of each species ($1 \leqslant \alpha \leqslant s$). The ions of each species α are distributed with the equilibrium density $\rho_\alpha(x)$ to be determined. The electrostatic potential ψ is expressed as:

$$\psi(x) = \int_V \sum_{\alpha=1}^{s} z_\alpha N_\alpha \frac{\rho_\alpha(x')}{|x - x'|}\,dx' + \psi_0(x). \tag{1}$$

For a rapid determination of the density $\rho_\alpha(x)$ one can simulate a MC random walk of a single ion of the species α in the potential $\psi(x)$ (created by polyion and other $N - 1$ ions) instead of producing conventional MC simulation of all ions in the volume V [14].

The simulation is carried out in the following way. An arbitrary initial distribution

of densities $\rho_\alpha^{(0)}(x)$ are chosen. The corresponding potential $\psi^{(0)}(x)$ is calculated according to Equation (1) with substitution $N_\alpha \to N_\alpha - 1$ and a random walk of a single ion of each species (in turn) is made which yields "corrected" distributions $\rho_\alpha^{(1)}(x)$. Inserting $\rho_\alpha^{(1)}(x)$ into Equation (1) we obtain an "improved" potential $\psi^{(1)}(x)$ and continue the iteration procedure until convergence.

If convergence does not occur it is possible to use a regularization procedure – to substitute at each iteration only a part of the distribution density:

$$\rho_\alpha^{(m+1)}(x) = (1 - \gamma)\rho_\alpha^{(m)}(x) + \gamma\rho_\alpha[\psi^{(m)}(x)], \tag{2}$$

where (m) is the iteration number, $\rho_\alpha[\psi^{(m)}(x)]$ is the distribution density obtained for potential $\psi^{(m)}(x)$, and $0 < \gamma \leqslant 1$ is the regularization parameter which determines the part of the density to be corrected at each iteration.

In the case of a symmetric polyion (a charge cylinder or a sphere of radius a in MC cell of radius R) a random walk of the chosen ion can be made in the interval $[a, R]$ (rather than in the whole three-dimensional space) with the addition to the energy of a term arising from the Jacobian of transition to new coordinates: $\ln(2\pi r)$ for the cylinder and $\ln(4\pi r^2)$ for the sphere.

It is obvious that the described algorithm is completely analogous to numerical solution of the PB equation by iteration method [18]. However it can be easily generalized to account for ionic correlations. This could be achieved by MC random walk of several (n) ions, n_α for each species, rather than a single ion [15].

2.2 Random Walk of Several Ions

Interactions among the chosen n ions are accounted for explicitly using for instance the charged hard sphere potential:

$$V_{ij} = \begin{cases} z_i z_j/|x_i - x_j| & |x_i - x_j| > (d_i + d_j)/2, \\ \infty & |x_i - x_j| < (d_i + d_j)/2, \end{cases} \tag{3}$$

where i, j enumerate the explicitly accounted ions, and d_i are their diameters. The effect of other $(N - n)$ ions is accounted for with the aid of the self-consistent field:

$$\psi_M^{(m)}(x) = \int_v \sum_{\alpha=1}^{s} z_\alpha(N_\alpha - n_\alpha) \frac{\rho_\alpha^{(m-1)}(x')\,dx'^3}{|x - x'|}. \tag{4}$$

We carry out a MC algorithm for n ions interacting with potential (3) in the "external" field $\psi^{(m)}(x) = \psi_0(x) + \psi_M^{(m)}(x)$ and perform the iteration procedure analogous to that described for a single ion.

Explicit account of only one ion (i.e., $n_\alpha = \delta_{\alpha\beta}$ – a single ion of each species moves randomly in turn) yields $\rho_\alpha \sim \exp(-z_\alpha\psi)$ and we obtain solution of the nonlinear PB equation, i.e., we come back to the previous case. Explicit account of all ions ($n_\alpha = N_\alpha$, $\psi_M = 0$) yields to the standard MC algorithm. Simulation with n ions accounts for most essential correlations. It was shown in Ref. [15] that $n \sim 3$–5 is sufficient to obtain results close to accurate MC (with explicit account of all ions) for the DNA-type polyion in 1 : 1 electrolyte. However further simulations showed some inconveniences of this method. Firstly the short range interactions (hard core) are accounted inadequately in this method. Secondly, if we have to take a large MC cell (in the case of small salt and/or DNA concentrations) the explicitly accounted for ions walk mostly in regions far from the polyion. So the charge distribution is calculated

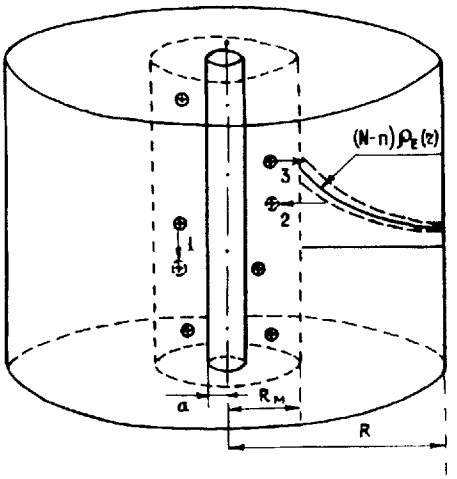

Figure 1 Division of the space around the polyion into two regions: internal and external. Types of MC steps: (1) displacement of ions; (2) their insertion; (3) their removal.

less accurately in its vicinity – the region where interionic correlations are the strongest and ρ_α should be determined most accurately. At the same time far from the polyion where $\psi < 1$, the SCF approximation is already valid and accurate account of correlations is not so necessary. Therefore we formulated and carried out the third version of the MC–SCF method [16] which is described in Section 3.

3 MC–SCF METHOD WITH DISTINGUISHED CLOSE VICINITY OF THE POLYION

3.1 General Theoretical Background

Consider a polyion, a cylinder or a sphere, of radius a placed in the centre of the MC cell of the corresponding shape and of radius R. In the vicinity of the polyion a concentric region of radius R_M, $a < R_M < R$ is distinguished (the internal zone). The MC random walk is performed only inside the cylinder (or sphere) of radius R_M (in the case of cylindrical polyion we consider only its finite part of height h with periodic boundary conditions along the Z axis of the cylinder). Ions outside the internal region (in the external zone) are accounted for by means of continuous density distribution (see Figure 1). In the internal region ions interact with potential of the type (3).

It is supposed that in the external region:

(1) the SCF approximation is valid;

(2) the potential and ion densities are cylindrically (spherically) symmetric functions, i.e., the influence of all the inhomogeneities of the charge distribution on the polyion are already smoothed at distances $r > R_M$ (Reference [19] shows that this supposition is well justified for an adequate choice of R_M).

Let the constant number of ions $N = \Sigma N_\alpha$, N_α for each particle species, fill a cell of volume V ($V = \pi(R^2 - a^2)h$ for the cylinder and $V = 4\pi(R^3 - a^3)/3$ for the

sphere). This volume is divided into two regions: internal (V_I) and external (V_E) by the separation surface of the radius R_M.

The initial expression for configurational integral of our system is standard:

$$Z = \frac{1}{\prod_{\alpha=1}^{s} N_\alpha!} \int \prod_{i=1}^{N} dx_i \exp(-\beta H\{x_i\}),$$

$$H\{x_i\} = (1/2) \sum_{i,j=1}^{N} V_{ij}(x_i, x_j) + \sum_{i=1}^{N} z_i \psi_0(x_i),$$

$$\beta = (kT)^{-1}.$$

For the case of uniformly charge cylinder we have

$$\psi_0(x) = -2\xi \ln(r),$$

where r is the distance between point x and cylinder axis, $\xi = l_B/b$ is the dimensionless linear charge density (b = charge separation). The integration over the whole cell is divided into two parts:

$$\int_v dx = \int_{v_I} dx + \int_{v_E} dx.$$

Using the bynomial expansion and transposition symmetry of the Hamiltonian we obtain:

$$\begin{aligned} Z &= \prod_{\alpha=1}^{s} \frac{1}{N_\alpha!} \prod_{i=1}^{N} \left(\int_{v_E} dx_i + \int_{v_I} dx_i \right) \exp(-\beta H\{x_i\}) \\ &= \prod_{\alpha=1}^{s} \left[\frac{1}{N_\alpha!} \sum_{n_\alpha=0}^{N_\alpha} C_{N_\alpha}^{n_\alpha} \prod_{i=1}^{n_\alpha} \left(\int_{v_I} dx_i \right) \prod_{j=n_\alpha+1}^{N_\alpha} \left(\int_{v_E} dx_j \right) \exp(-\beta H\{x_i, x_j\}) \right] \\ &= \prod_{\alpha=1}^{s} \left(\sum_{n_\alpha=0}^{N_\alpha} \frac{1}{n_\alpha!} \right) \int_{v_I} \prod_{i=1}^{n} dx_i \exp(-\beta H_{in}\{x_i\}) Z_E(n, \{x_i\}), \end{aligned} \tag{5}$$

where

$$H_{in}\{x_i\} = (1/2) \prod_{i,j=1}^{n} V_{ij}(x_i, x_j) + \sum_{i=1}^{n} z_i \psi_0(x_i)$$

$$Z_E(n, \{x_i\}) = \prod_{\alpha=1}^{s} \frac{1}{(N_\alpha - n_\alpha)!} \int_{v_E} \prod_{i=n}^{N} dx_i \times \exp\left[-\beta \left(\sum_{k=1}^{n} \sum_{j=n+1}^{N} V_{jk} + \frac{1}{2} \sum_{j,k=n+1}^{N} V_{jk} + \sum_{k=n+1}^{N} z_i \psi_0(x_i) \right) \right].$$

Here n_α is the number of ions of α-species and $n = \sum_{\alpha=1}^{s} n_\alpha$ is the total number of ions in the internal zone. The index N or n in sums or products implies summation or multiplication over all species; indices N_α or n_α correspond to summation or multiplication over species δ.

n_α in Equation (5) is a variable. Accordingly simulation includes three types of MC steps: ion movement within the internal region; insertion of an ion to and its removal from the internal region.

Z_E is the configuration partition function of the ions in the external region at condition that coordinates $\{x_i\}$, $i = 1, \ldots, n$ of the ions in the internal region are fixed. Now we introduce the free energy of the external region:

$$F_{ex}(n, \{x_i\}) = kT \ln (Z_E),$$

which can be presented in the following form:

$$F_{ex} = U_i + U_e + U_p - TS. \tag{6}$$

Here U_i, U_e and U_p are contributions to the internal energy: U_i corresponds to interaction of the external ions with the internal ions, U_e corresponds to interaction of the external ions with each other, and U_p corresponds to interaction of external ions with the polyion. S is the entropy of the external distribution.

For the calculation of F_{ex} we apply suppositions (1) and (2). In as much as distribution density in the external region is supposed to be symmetric (condition 1) the electrostatic interaction energy of the external charge with the internal ions does not depend on the ion configuration $\{x_i\}$ inside radius R_M and is determined only by the value of their total charge. Let $\rho_{E_\alpha}(r)$ be the normalized on unity distribution density of the αth species in the external region. The potential created by the latter is expressed (in the cylindrical case) as:

$$\psi_{E_\alpha}(r) = 4\pi \left[\ln\left(\frac{r}{R}\right) \int_{R_M}^{r} r' \rho_{E_\alpha}(r')\, dr' + \int_{r}^{R} r' \rho_{E_\alpha}(r') \ln\left(\frac{r'}{R}\right) dr' \right]. \tag{7}$$

In the SCF approximation for internal energy terms in Equation (6) we can write:

$$\begin{aligned} U_i &= \sum_{\alpha=1}^{s} z_\alpha n_\alpha \sum_{\gamma=1}^{s} z_\alpha (N_\alpha - n_\alpha) \psi_{E_\alpha}(R_M) \\ U_e &= \sum_{\alpha,\gamma=1}^{s} \left[z_\alpha (N_\alpha - n_\alpha) z_\gamma (N_\gamma - n_\gamma)/2 \int_{R_M}^{R} 2\pi r \psi_{E_\alpha}(r) \rho_{E_\alpha}(r)\, dr \right] \\ U_p &= \sum_{\alpha=1}^{s} z_\alpha (N_\alpha - n_\alpha) \int_{R_M}^{R} 2\pi r 2\xi \ln (r) \rho_{E_\alpha}(r)\, dr. \end{aligned} \tag{8}$$

For the entropy the standard expression in canonical ensemble is taken as a basis:

$$S = k < \ln (\rho_E(r_{n+1}, \ldots, r_N)) >_{\rho_E(r_{(n+1)}, \ldots, r_N)}. \tag{9}$$

Averaging in Equation (9) is made over the full (multiparticle) distribution function in the external region $\rho_E(r_{(n+1)}, \ldots, r_N)$. In the SCF approach ρ_E is a product of single particle distribution functions:

$$\rho_E(r_{n+1}, \ldots, r_N) = \prod_{\alpha=1}^{s} (N_\alpha - n_\alpha)! \prod_{i=n_\alpha+1}^{N_\alpha} \rho_{E_\alpha}(r_i). \tag{10}$$

Terms $(N_\alpha - n_\alpha)!$ arise due to transposition symmetry of the Hamiltonian. Substituting Equation (10) into Equation (9) we obtain:

$$S = -k \sum_{\alpha=1}^{s} \left[(N_\alpha - n_\alpha) \int_{R_M}^{R} 2\pi r \rho_{E_\alpha}(r) \ln (\rho_{E_\alpha}(r)) - \ln (N_\alpha - n_\alpha)! \right]. \tag{11}$$

Formulae (5)–(8), (11) provide us with the transition probabilities for MC procedure with variable number of ions in the internal zone.

3.2 Determination of the Nonideal Contribution to the chemical potential

In calculating the free energy in the SCF approximation according to Equations (7)–(11) we neglect ion correlations in the external region as in Ref. [16]. Strictly it could be written:

$$F_{ex} = F_{id} + F_{ni}, \tag{12}$$

where F_{id} is the free energy in SCF approach (according to Equation (6) with Equations (8) and (11) for energy and entropy contributions); and F_{ni} is the "non-ideal" part which is associated with ionic correlation in the external region. It should be noted that this part of the free energy exists always independently of how great is the radius R_M: in the limit $R_M \to \infty$ F_{ni} tends to the free energy of the primitive model of the electrolyte.

Steps with removal and insertion of a single particle yield to the following change of the free energy of the external region:

$$\Delta F_{ex} = F_{ex}(n+1) - F_{ex}(n) = \mu = \mu_{id} + \mu_{ni}, \tag{13}$$

where μ is the chemical potential. To make formulae simple we omit in this section the subscript α keeping in mind that all the expressions are valid for each ion species separately.

μ_{id} can be calculated as a difference of free energies according to Equations (7)–(11). The nonideal part of the chemical potential of ions α species at given ion concentrations of all species can be obtained from simulation of simple electrolyte in μVT-ensemble [20] (these results were used in Ref. [21] for MC-simulation of the electric double layer at a flat wall). In our approach the estimation of μ_{ni} can be included into the suggested algorithm.

Consider a case when R_M is so great that one can write $\psi(R_M) = 0$. Correspondingly in the external region we have a homogenous ion distribution with the total charge density being equal to zero and, according to Equation (8)

$$U_e = U_i = U_p = 0, \tag{14}$$

Since initially the correct μ_{ni} is unknown we introduce some quantity μ^* which we use in calculation of ΔF_{ex} according to Equation (13).

Let $P(n, \{x_i\})$ be the probability density corresponding to n ions in the internal region with coordinates $\{x_i\}$. Then for the ratio of probabilities (see Equation (5)) we obtain:

$$\frac{p(n+1, \{x_i\}, x_{n+1})}{p(n, \{x_i\})} = \frac{1}{n+1} \exp[-\beta(H_{in}(n+1) - H_{in}(n)] - \beta[F_{ex}(n+1) - F_{ex}(n)]. \tag{15}$$

Using Equation (14) and the assumption of homogeneous distribution in the external region we obtain:

$$-\beta\Delta F_{ex} = S(n+1) - S(n) - \beta\mu^* = \ln[(N-n)/V_E] - \beta\mu^*. \tag{16}$$

Equations (15) and (16) yield:

$$P(n+1, \{x_i\}, x_{n+1})(n+1) = P(n, \{x_i\}) \frac{N-n}{V_E} \exp(-\beta\Delta H_{in}) \exp(-\beta\mu^*).$$

Now we average both sides of this equation over $\{x_i\}$. In the left side we obtain

$P(n+1)\rho(x_{n+1})$ where $P(n)$ is the probability for the number of particles in the internal region to be n, $\rho(x_{n+1})$ is the density distribution in the internal region (strictly speaking it is valid as long as the single particle distribution functions does not depend on n). So after averaging:

$$P(n+1)\rho(x_{n+1}) = P(n)\frac{N-n}{V_E}\exp(-\beta\mu^*)\langle\exp[-\beta\Delta H(x_{n+1})]\rangle. \quad (17)$$

It can be considered that the equilibrium value of the particle number in the internal region corresponds to the maximum of $P(n)$ [$dP/dn = 0$, or $P(n) = P(n+1)$]. Averaging $\langle \ldots \rangle$ in Equation (17) yields actually $\exp[\beta\mu(x_{n+1})]$ (Windom formula [22]). If $x \to R_M$, μ is the value of chemical potential in the internal region at the boundary which should be equal to chemical potential in the external region μ_{ni}. So if we have started with $\mu^* = \mu_{ni}$, we should obtain:

$$\rho_{in}(R_M) = \frac{N-n}{V_E} = \rho_{ex},$$

i.e., distribution density is equal on both sides of the border R_M.

If μ_{ni} is unknown and we make simulation with some $\mu^* \neq \mu_{ni}$ (initially one can put $\mu^* = 0$) we should obtain a jump of density at the border:

$$\rho_{in}/\rho_{ex} = \exp[\beta(\mu_{ni} - \mu^*)]. \quad (18)$$

After obtaining this jump we can correct μ^* according to Equation (18) and carry out a further simulation with the corrected μ^*. It could be noted that such a procedure formally looks like a mechanical fitting of densities in the outer and inner regions: if $\rho_{in} < \rho_{ex}$ then in accordance with Equation (18) we ought to decrease μ^* which in its turn according to Equation (13) results in augmenting of transition probability of insertion and correspondingly decrease of transition probability for removal.

In the case when the border R_M is situated sufficiently close to the polyion (this is the case we are mainly interested in), one can carry out the same procedure in which ρ_{in} and ρ_{ex} are densities at the border on both of its sides. As a justification of such a procedure an assumption may serve that the density should be continuous and this is just what the procedure does provide.

3.3 Simulation Algorithm

Since for calculation of transition probabilities we should already know in advance the density distributions of ions, which are in their turn the aim of our simulation, the simulation as a whole is organized as an iteration procedure: a certain distribution is taken as an initial one and then it is being corrected in the course of simulation. In principle the result should not depend on the initial distribution though evidently it should be chosen as close to the equilibrium as possible. For instance one can use for this purpose the numerical solution of the PB equation. So the proposed calculational scheme is the following.

(1). A numerical solution of the PB equation is obtained in the whole MC cell of radius R. Its solution gives the initial distribution of densities for all ion species in the outer region $\rho_{E_\alpha}(r)$ and initial "average" number of ions of each species in the internal region $\langle n_\alpha^{(0)}\rangle$. In the course of numerical solution of the PB equation with the aid of iteration procedure (Section 2) an optimal value of regularization parameter γ is also chosen. Ent $\langle n_\alpha^{(0)}\rangle$ ions of each species are inserted into internal region.

Now the main iteration procedure starts which includes the following steps (pp. 2–3).

(2). In the internal region the MC procedure with three types of steps is carried out: shifts of particles, their insertion and removal. Each MC step starts with trial of the transition type (as a rule attempts to shift a particle were made with probability 0.8, and to remove or insert – with 0.1).

For shifts of particles a conventional NVT-ensemble procedure is used. It should be noted that for shifted ions one needs to calculate the interaction energy only with ions in the internal region and with polyion since their energy in the field of the external symmetric distribution does not change (condition of symmetry of external distribution – Section 3.1). If the shifted ion crosses the border (cylinder or sphere of radius R_M) such attempt is rejected (transition to the external region is carried out by a special type of step – removal of an ion is necessary to satisfy the detailed balance principle). Periodic boundary conditions along the cylinder axis are used; interactions with periodic images of ions out of the basic MC cell are calculated by means of Evald procedure (see Appendix 1).

If we remove (insert) an ion of species α out of (into) the internal region a term $z_\alpha \rho_{E_\alpha}^{(m)}(r)$ is added to (subtracted from) the external distribution function;

$$(N_\alpha - n_\alpha)\rho_{E_\rho}^{(m)}(r) \to (N_\alpha - n_\alpha \pm 1)\rho_{E_\alpha}^{(m)}(r).$$

For MC steps with insertion and removal of ions transition probabilities are determined from the following expression (see e.g. Ref. [10]):

$$\frac{P(n_\alpha \to n_\alpha + 1)}{P(n_\alpha + 1 \to n_\alpha)} = \frac{V_I}{n_\alpha + 1}\exp[-\beta(\Delta H_{in} + \Delta F)], \tag{19}$$

where ΔH_{in} is the change of interaction energy of ions in the internal region, ΔF is the change of the free energy of the external region, and V_I is the internal volume. These values are calculated beforehand and kept in the memory. During MC simulation ion distribution and mean number of ions in the internal region $\langle n_\alpha \rangle_{MC}^{(m)}$ are calculated. Each iteration includes $\sim 10_{MC}^5$ steps.

(3). Values associated with charge distribution in the external region are being corrected:

(a) charge distribution of all species of ions in the outer region:

$$\rho_{E_\alpha}^{(m+1)}(r) = (1 - \gamma)\rho_{E_\alpha}^{(m)}(r) + \gamma\rho_{E_\alpha}[\psi^{(m)}(r)] \tag{20}$$

where

$$\rho_{E_\alpha}[\psi^{(m)}(r)] = C\exp[-z_\alpha\psi^{(m)}(r)],$$

$0 < \gamma \leqslant 1$ is the regularization parameter, C is the normalizing constant, (m) is the iteration number, and $\psi^{(m)}(r)$ is the full electrostatic potential in the external region:

$$\psi^{(m)}(r) = \sum_{\alpha=1}^{s}(N_\alpha - \langle n_\alpha \rangle^{(m)})\psi_{E_\alpha}^{(m)}(r) - 2\left(\xi - \sum_{\alpha=1}^{s} z_\alpha \langle n_\alpha \rangle^{(m)}/h\right)\ln(r). \tag{21}$$

The first term in Equation (21) expresses the potential of ions in the outer region, and the second term expresses the potential of the polyion and ions in the internal region; in this case the internal region is considered as a cylinder of the radius R_M with the

linear density

$$\left(\xi - \sum_{\alpha=1}^{s} z_\alpha \langle n_\alpha \rangle^{(m)}/h\right).$$

(b) mean number of ions in the internal region:

$$\langle n_\alpha \rangle^{(m)} = (1 - \gamma_2)\langle n_\alpha \rangle^{(m-1)} + \gamma_2 \langle n_\alpha \rangle_{\mathrm{MC}}^{(m)},$$

where $0 < \gamma_2 \leqslant 1$ is the regularization parameter for number of ions (number of ions in the internal zone is also corrected partially). We usually take $\gamma_2 = \gamma^{1/2}$.

(c) The nonideal part of the chemical potential is being corrected beginning from the 4–6th iteration after ionic density distributions have gained some equilibrium. Moreover in order to decrease the influence of fluctuations $\rho_{\mathrm{in}}(R_{\mathrm{M}})$ (this quantity is obtained from MC averaging) the correction to the chemical potential is also added gradually – by parts. In this work we use:

$$\mu_{\mathrm{ni}}^{(m+1)} = \mu_{\mathrm{ni}}^{(m)} + \gamma^{1/2} \ln[\rho_{\mathrm{in}}^{(m)}(R_{\mathrm{M}})/\rho_{\mathrm{ex}}^{(m)}(R_{\mathrm{M}})]. \tag{22}$$

Then the integrals (8) are recalculated and the next iterations starts.

(4). When the results obtained at each next iteration cease to change a series of 10–20 iterations is carried out. The resulting data are averaged and the obtained results are considered to be final. Dispersion based on this series yields the estimate of the statistical error.

If the PB solution was used as an initial approximation the establishing of equilibrium requires about 5–10 iterations.

For spherical polyions, formulae (7), (8), (11) and (21) are substituted by:

$$\psi_{\mathrm{E}_\alpha}(r) = 4\pi\left[\frac{1}{r}\int_{R_{\mathrm{M}}}^{r} r'^2 \rho_{\mathrm{E}_\alpha}(r')\,\mathrm{d}r' + \int_{r}^{R} r'\rho_{\mathrm{E}_\alpha}(r')\,\mathrm{d}r'\right], \tag{7a}$$

$$U_i = \sum_{\alpha=1}^{s} z_\alpha n_\alpha \sum_{\gamma=1}^{s} (N_\gamma - n_\gamma)\psi_{\mathrm{E}_\gamma}(R_{\mathrm{M}}),$$

$$U_e = \sum_{\alpha,\gamma=1}^{s}\left[z_\alpha(N_\alpha - n_\alpha)z_\gamma(N_\gamma - n_\gamma)/2)\int_{R_{\mathrm{M}}}^{R} 4\pi r^2 \psi_{\mathrm{E}_\gamma}(r)\rho_{\mathrm{E}_\alpha}(r)\,\mathrm{d}r\right] \tag{8a}$$

$$U_p = \sum_{\alpha=1}^{s} z_\alpha(N_\alpha - n_\alpha)\int_{R_{\mathrm{M}}}^{R} 4\pi r^2 (Q/r)\rho_{\mathrm{E}_\alpha}(r)\,\mathrm{d}r,$$

$$S = -k\sum_{\alpha=1}^{s}\left[(N_\alpha - n_\alpha)\int_{R_{\mathrm{M}}}^{R} 4\pi r^2 \rho_{\mathrm{E}_\alpha}(r)\ln[\rho_{\mathrm{E}_\alpha}(r)]\right] + \ln(N_\alpha - n_\alpha)! \tag{11a}$$

$$\psi^{(m)}(r) = \sum_{\alpha=1}^{s}(N_\alpha - \langle n_\alpha \rangle^{(m)})\psi_{\mathrm{E}_\alpha}^{(m)} - \left(Q - \sum_{\alpha=1}^{s} z_\alpha \langle n_\alpha \rangle^{(m)}\right)/r. \tag{21a}$$

4 METHODOLOGICAL CALCULATIONS

4.1 Choice of Regularization Parameter

Convergence of the iteration process depends on the choice of γ, the regularization

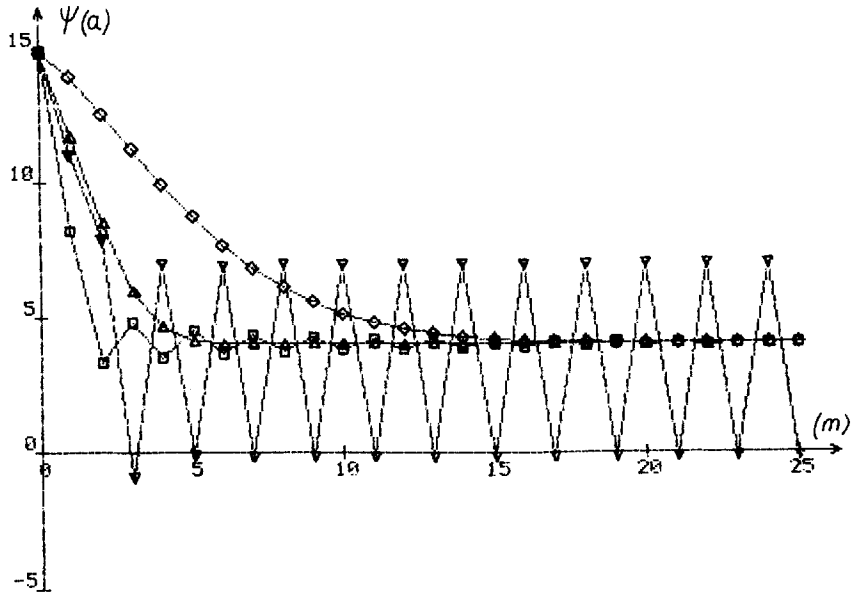

Figure 2 Process of convergence of the MC–SCF method (first version). Shown is potential at the polyion surface *vs* iteration number at various regularization parameters γ: ◇, 0.02; △, 0.05; □, 0.1; ▽, 0.2. Cylindrical polyion, $a = 1$ nm, $R = 27$ nm, $\xi = -4.2$.

parameter determining the part of density to be corrected at each iteration: the smaller is γ, the smaller part of the density is being corrected (2), (20). Its influence on the convergence process is demonstrated in Figure 2 for surface potential of the cylindrical polyion (in this case the first variant of the MC–SCF method with explicit account of a single ion was used with constant initial distribution: $\rho^{(0)}(r) = \text{const.}$). It is seen that for large γ (e.g., $\gamma = 0.2$ for the condition of Figure 2) the iteration process has an oscillatory character and does not converge. Decreasing γ we gain convergence but oscillations still hold. For very small γ convergence is monotonous though very slow. So there exists an optimal value of γ for which equilibrium is achieved after several (4–6) iterations.

For other variants of the MC–SCF method the dependence of convergence rate on γ is of the same character. So it is possible to make an optimal choice of γ automatically inside the program. In practical calculations the regularization parameter is usually chosen in the beginning of simulations while solving the PB-equation. The same value of γ is used later in the course of the main simulation.

It is evident that ultimate results (providing that convergence exists) should not depend either on γ or on the initial density distribution. In the cylindrical case acceptable values of γ can be obtained by an empirical formula:

$$\gamma = 1/(\xi + c_0 \pi R^2/2).$$

Here ionic strength c_0 and radius R are expressed in dimensionless units.

4.2 Choice of Intermediate Radius R_M

Numerical results obtained in calculations with different values of R_M are given in

Table 1. They are densities of mono and divalent counterions and the potential at the polyion surface. The extreme cases are also presented – solution of the PB equation (formally $R_M = a$) and ordinary MC-calculation in the whole MC-cell ($R_M = R$). We also indicate average number of ions in the internal region. It can be seen (from strings marked by "1") that for $R_M = 3.1$ nm the results are already the same as those for $R_M = R$ (full MC) though in the former case the number of explicitly accounted ions is about ten times less than for full MC.

Data obtained by MC–SCF method with no account for the chemical potential correction is also represented in Table 1 ($\mu_{ni} = 0$ as it was in Ref. [16]; in Table 1 these results are labelled by "2"). It is seen that in this case a small deviation (up to 5%) from the full MC data ($R_M = R$) is observed. Calculations showed that these deviations become noticible for concentrations of the divalent ions exceeding 0.1 M. It should be pointed out however that the account of the chemical potential correction requires several additional iterations to establish the equilibrium. It results also in a certain increase of the statistical error since the correction is determined from the ion density value at the border of the internal region [see Equation (22)]. In order to decrease the error the number of MC steps per iteration should be increased. Lines in Table 1 labeled by "1" are obtained after 3×10^6 MC steps (for all iterations) and those labeled by "2" – after 10^6 MC steps.

4.3 Choice of the MC-cell Height

Dependence of results (the same quantities as in Table 1) on MC-cell height is demonstrated in Table 2. The data show that for $h > 7$ nm the results seem to be independent on h. This value of the MC cell height can be considered as optimal for conditions corresponding to the set of input parameters (Table 2).

5 RESULTS FOR A CYLINDRICAL POLYION

5.1 Potential and Density of Ions at the Surface

In all calculations the cylindrical polyion had parameters of the B-form of DNA in water solution at room temperature: radius $a = 1$ nm and dimensionless linear charge density $\xi = 4.2$.

Figure 3 presents simulation results for surface potential dependence on the salt concentration compared with PB data for monovalent salt (1 : 1 electrolyte; data is taken from the previous paper [15]) and divalent salt (2 : 2 electrolyte). It is seen that PB-equation gives higher values of the surface potential in both cases. However for monovalent salt this deviation is small (not more than 10%) while for divalent salt it becomes considerably greater.

Such difference is evidently caused by the fact that for monovalent ions their diameter (with the account of hydration shell) – 0.42 nm is close to their Bjerrum length (0.71 nm), i.e. even at closest approach distance the Coulomb energy $(ze)^2/\varepsilon d$ is not much higher than thermal energy (kT). So the Coulomb correlations between ions are not great in this case and the PB equation which ignores them at all yields comparatively good results. For divalent ions the Bjerrum length is four times greater and interionic correlation effects become significant. These effects are adequately accounted for only in simulations.

Figure 4 presents counterion charge density at the surface of the polyion for a

Table 1 Some simulation results for cylindrical polyion of DNA-type immersed in 2:1:1 electrolyte obtained at various intermediate radii R_M. a = 1.nm, R = 27 nm, h = 7.1 nm, ξ = −4.2, number of ions of each species: N_{+2} = 30, N_{+1} = 82, N_{-1} = 100. 1, present algorithm; 2, without correction of the chemical potential (μ_{ni} = 0, as in Ref. [16]). Densities of counterions at the polyion surface are given in dimensionless units (number of ions per l_b^3).

R_M (nm)		1.0(a)	1.4	2.0	3.1	5.6	10.0	27.0 (R)
$\psi(a)$	1	4.04	3.28 ± 0.02	2.86 ± 0.02	2.81 ± 0.04	2.78 ± 0.05	2.80 ± 0.02	2.79 ± 0.03
	2		2.94 ± 0.02	2.81 ± 0.02	2.89 ± 0.03	2.88 ± 0.05	2.94 ± 0.05	
$\rho_{2+}(a)$	1	0.96	1.21 ± 0.01	1.214 ± 0.01	1.215 ± 0.02	1.23 ± 0.02	1.21 ± 0.03	1.2 ± 0.1
	2		1.25 ± 0.02	1.225 ± 0.02	1.18 ± 0.04	1.24 ± 0.04	1.24 ± 0.1	
$\rho_{1+}(a)$	1	0.093	0.08 ± 0.003	0.07 ± 0.003	0.07 ± 0.004	0.066 ± 0.005	0.067 ± 0.006	0.068 ± 0.01
	2		0.082 ± 0.005	0.065 ± 0.005	0.073 ± 0.008	0.08 ± 0.01	0.09 ± 0.02	
$\langle n \rangle$		0	16.1	19.3	21.8	28.4	47.2	212

Table 2 Simulation results for cylindrical polyion of DNA-type immersed in 2 : 1 : 1 electrolyte obtained at various MC cell heights h (concentrations of each ion species hold fixed). $a = 1$ nm, $R = 7.1$ nm, $R_M = 2.8$ nm, $\xi = -4.2$, mean concentration of each species: $c_{+2} = 0.062$ M, $c_{+1} = 0.155$ M, $c_{-1} = 0.217$ M.

h (nm)	1.36	3.4	6.8	10.2	13.6	17.0
$\psi(a)$	1.54 ± 0.02	1.25 ± 0.02	1.08 ± 0.03	1.06 ± 0.04	1.09 ± 0.04	1.10 ± 0.04
$\rho_{2+}(a)$	1.0 ± 0.01	1.193 ± 0.02	1.30 ± 0.02	1.28 ± 0.02	1.29 ± 0.02	1.30 ± 0.03
$\rho_{1+}(a)$	0.32 ± 0.01	0.28 ± 0.01	0.255 ± 0.02	0.23 ± 0.02	0.24 ± 0.02	0.23 ± 0.02

mixture of three species of ions of valency +1, +2 (counterions) and −1 (coions). Its dependence on divalent ions fraction at three fixed values of the total ionic strength is shown. Analysis of the results yields to the following conclusions. At small fractions of divalent ion concentration (up to 10%) the (+2) ion gradually "squeeze" the monovalent ions off the polyion surface and surface density of (+2) ions rapidly increases with their mean concentration. At further increase of c_{+2}/c ratio (up to 40–50%) the (+1) ions are squeezed off the polyion surface completely, density of (+2) ions seizes to grow gaining saturation. The total surface density of the counterions weakly depends on the ionic strength and holds very high (several M/l) even at very low salt concentration.

5.2 Application to Flexible Polyelectrolyte Chains

It is assumed that the polyelectrolyte of the DNA-type can be considered as being

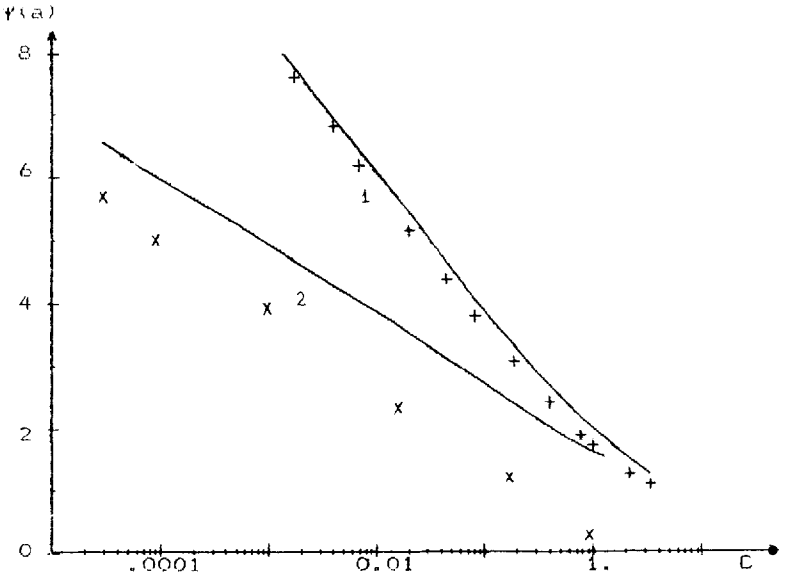

Figure 3 Potential at the cylindrical polyion surface for 1 : 1 and 2 : 2 electrolyte; dependence on the ionic strength. $\xi = -4.2$, $a = 1$ nm. Points, MC–SCF method; lines, PB approximation. (1) 1 : 1 electrolyte; (2) 2 : 2 electrolyte.

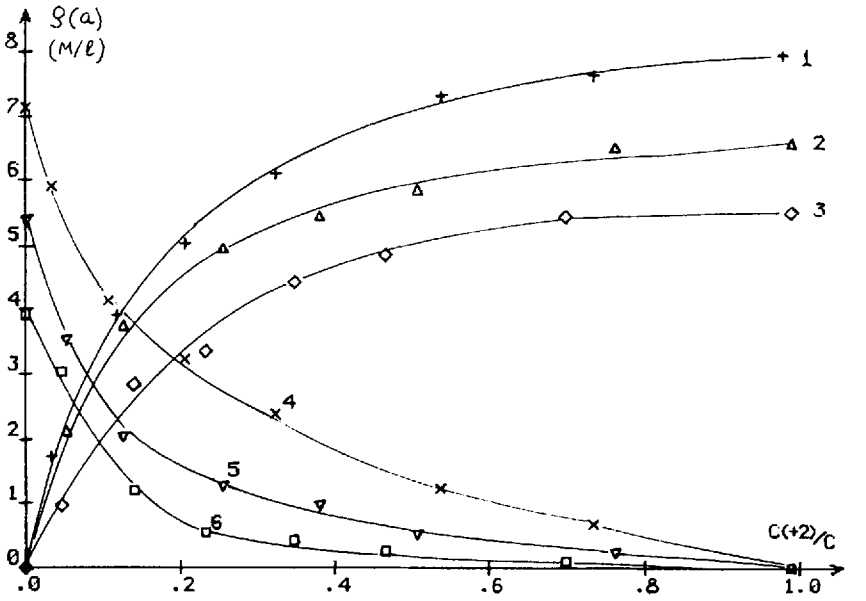

Figure 4 Counterion densities on the surface of the cylindrical polyion; dependence on the divalent ion fraction. $\xi = -4.2$, $a = 1$ nm. (1–3) divalent ions; (4–6) monovalent ions; total ionic strengths: (1,4) $c = 1$ M/l; (2,5) $c = 0.1$ M/l; (3,6) $c = 0.005$ M/l. Lines are given to guide the eye.

rigid only for distances not exceeding its persistence length. Macromolecules of greater length form a coil. Electrostatic repulsion of polyion charge groups results in augmentation of the coil size caused by two factors – the increase of the persistent length and growth of the effective excluded volume. For DNA the increase of the persistent length is noticeably displayed only at extremely low concentration (lower than 10^{-3} M/l [23]; computer simulation results show that it is so even for sufficiently more flexible polyelectrolytes [24]). So it is possible to estimate the value of the polyelectrolyte swelling due to the increase of the effective excluded volume. Let us consider in accordance to Alexandrowicz [25] that the effective electrostatic radius of the DNA coil is determined by the condition that at this distance the reduced electrostatic potential (i.e. the ratio of potential energy of repulsion to the average heat energy) is equal to 1. This way we substitute the polyelectrolyte chain by an effective noncharged chain with the diameter D, determined by the condition:

$$\psi(D/2) = 1.$$

The value of D denotes an average distance of closest approach of two different pieces of a polyelectrolyte chain in solution.

In this case the effective excluded volume of a segment according to Refs. [25, 26] is (for $D \ll l$, l being Kuhn segment length):

$$w = \tfrac{1}{2}\pi D l^2. \tag{23}$$

The corresponding value of the dimensionless excluded volume parameter

$$z = [3/2\pi l^2)^{3/2} w N^{1/2} = [(27/32)(L/\pi l^3)]^{1/2} D$$

(L is the contour length of the macromolecule).

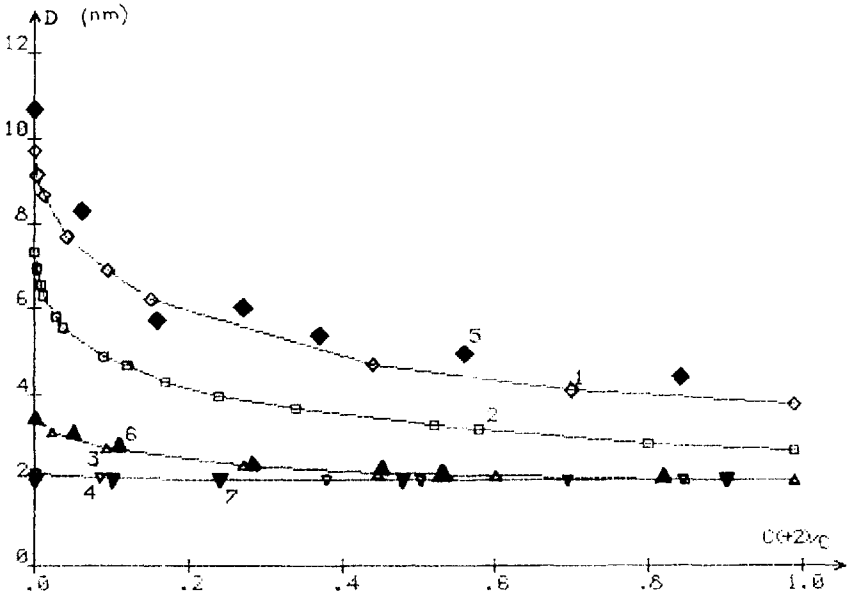

Figure 5 Effective electrostatic radius of DNA at varous ionic strength and divalent ion fractions. (1–4) MC–SCF calculations, lines are given to guide the eye; (5–7) calculated by formula (25) from intrinsic viscosity data [28]. Total ionic strength: (1,5) $c = 0.005$ M/l; (2) $c = 0.01$ M/l; (3,6) $c = 0.1$ M/l; (4,7) $c = 1$ M/l.

For the expansion factor α one can use the Fixman expression [27]:

$$\alpha^3 = 1 + 2z = 1 + [27L/(8\pi l^3)]^{1/2} D. \tag{24}$$

Using (24) in the expression of the average square distance between the ends of the polymer chain $\langle h^2 \rangle = \alpha l L$ we obtain for the intrinsic viscosity:

$$[\eta] = \frac{\Phi \langle h^2 \rangle^{3/2}}{M} = \frac{\Phi}{M}(lL)^{3/2} + \frac{\Phi}{M}(27/8\pi)^{1/2} DL^2 \tag{25}$$

(Φ = Flory constant, M = molecular weight).

Our simulation method yields the value of D. The same value can be obtained from the experimental data on intrinsic viscosity using formula (25).

Figure 5 shows dependence of D on the fraction of divalent ions at various total ion concentrations in comparison with the same dependences calculated according to Equation (25) on the basis of intrinsic viscosity data from the work of Kasyanenko *et al.* [28] for DNA of the mass $M = 9$ MDa, with the use of values $l = 75$ nm and $\Phi = 1.5 \times 10^{21}$ M^{-1}). Choice of the value of Flory constant is made so as to obtain coincidence with the experiment at the ionic strength 1 M/l when the electrostatic interactions has practically no influence and the viscosity is not changed with substitution of monovalent ions by divalent ones. It should be also pointed out that this value of Φ corresponds to existing estimates of the Flory constant for DNA in the range of $(1.1–2.9) \times 10^{21}$ M^{-1} [23, 26].

The compared results display very good agreement and show that the divalent ions have the strongest influence on the conformational properties of DNA at low ionic

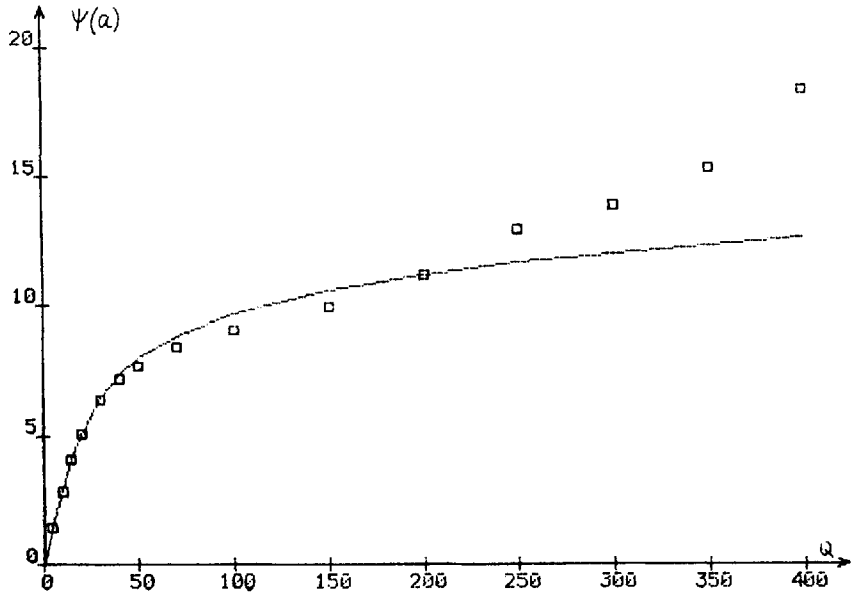

Figure 6 Potential at the surface of the spherical polyion immersed in 1 : 1 electrolyte; the dependence on the polyion charge. $a = 2$ nm, $R = 20$ nm, number of coins $N_{+1} = 10$. Points, MC–SCF method; line, PB approximation.

strengths. Presence of divalent ions in this case yields to sufficiently closer approach of distant parts of the DNA molecule. At high ionic strength substitution of monovalent ions by divalent ions has no significant influence.

6 RESULTS FOR A SPHERICAL POLYION

Spherical polyelectrolytes – proteins, micelles hold usually a charge of some tens of elementary units and have radius about several nanometers [8, 9]. Such parameters were used in our simulations.

Figure 6 shows dependence of the potential at the surface of the spherical polyion on its charge in the case of monovalent ionic surrounding. The polyionic radius, the size of MC cell and the number of ions of added salt are kept constant, the number of "own" counterions are being changed to compensate the increase of the polyionic charge. Comparison with PB approximation shows that for $Q < 200$ there is practically no difference between MC and PB results, however for $Q > 200$ the MC potential starts significantly to exceed that of PB. This effect is caused by sterical repulsion of ions. For a very high polyionic charge and a not too low polyionic concentration (i.e., not too large R) almost all the excessive counterions are concentrated on the polyionic surface. The maximum number of ions which can be distributed on the polyion surface in closest package for the used set of parameters is equal to $4\pi^2/d^2 = 274$. So if the number of ions on the polyion surface exceeds ~ 200 it is impossible for them to be distributed in the first coordinate layer which prevents its further growth thus resulting in the increase of the surface potential. It

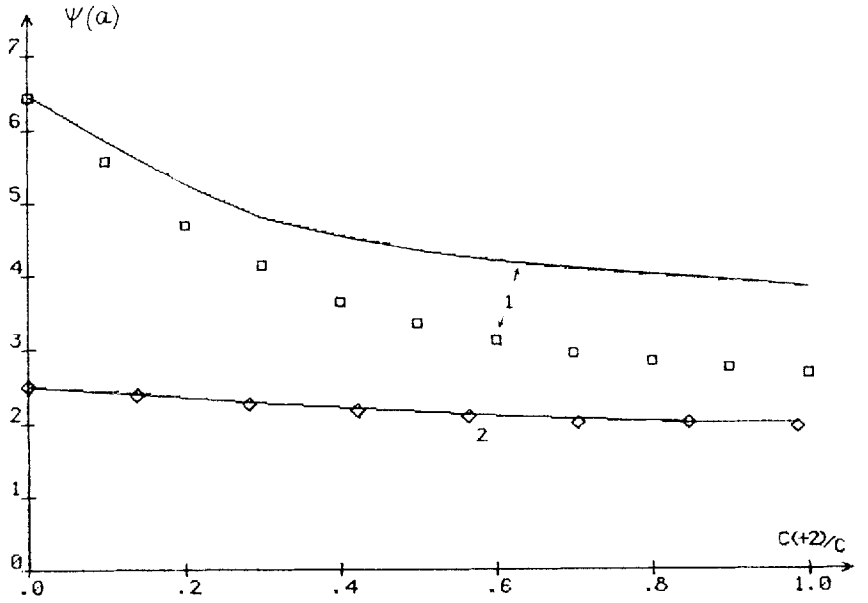

Figure 7 Potential at the surface of the spherical polyion in prescence of mono- and divelent counterions. $a = 2$ nm, $R = 20$ nm, number of coions $N_{+1} = 60$ (ionic strength 0.0032 M). Points, MC–SCF method; lines, PB approximation; (1) $Q = 40e$, (2) $Q = 10e$.

should be noted however that such a set of parameters is not realistic. Though the charge of micelles or colloid particles could reach several hundred of units the corresponding radius usually becomes also great – much greater than in the discussed case (Figure 6) and hence the steric repulsion could not be of any importance.

Figures 7 and 8 show respectively potential and counterion charge density at the surface of the spherical polyion in the case when the solution contains mono- and divalent counterions (analogous to the case of Figure 4 for the cylindrical polyion). The polyion charge was $10e$ and $40e$ and radius 2 nm. For the first case ($Q = 10e$) deviation of our results from PB approximation is small – less than 5%.

The increase of the polyion charge up to 40e makes the surface charge density equal to that for the DNA cylindrical model, $\sigma = 0.4$ in Bjerrum units. In this case the PB approximation appears to be justified only for monovalent ions ($c_{+2}/c = 0$); in presence of divalent ions PB approximation yields to increased values of the potential and density of the monovalent ions at the surface and lowered values for the density of the divalent ions – the result analogous to that for the cylindrical case [17].

7 CONCLUSION

In conclusion it could be instructive to trace some analogies between the MC–SCF method suggested here and other approaches.

On one hand the MC–SCF procedure formally is a routine μVT-ensemble simulation with a special dependence $\mu(n)$ accounting for inhomogeneous field in the external region [Equation (8)]. There can be also traced a parallelism (though not

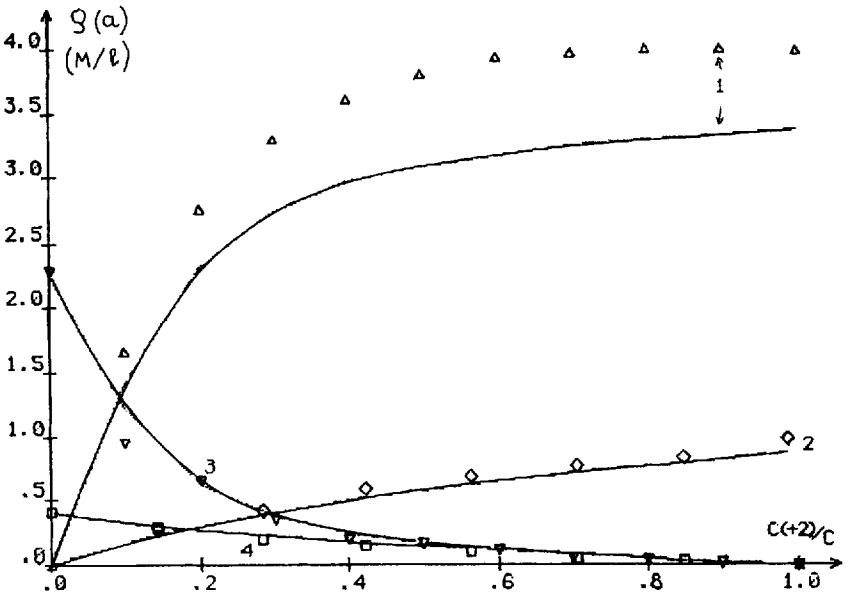

Figure 8 Counterion densities at the surface of the spherical polyion. Parameters are the same as in Figure 7. (1,2) divalent ions, (3,4) monovalent ions (for this case ion densities are multiplyed on factor 10); Points, MC–SCF method; lines, PB approximation. (1,3) $Q = 40e$, (2,4) $Q = 10e$.

complete) between the MC–SCF method and the algorithm of Panagiotopoulos for Gibbs ensemble MC simulations [29], especially in its recent variant [30]: division into two regions, exchange of particles between them, possible analytical or approximate treatment of one of the systems.

On the other hand it should be pointed out that the idea of separation of the space around the polyion into two regions – the internal (close to polyion) with a detailed simulation and external, was suggested first by Clementi [31]. According to Clementi in the internal region ions and water molecules were accounted explicitly, the external space contains only ions with effective parameters accounting implicitly for solvent. Clementi's method is aimed at adequate and detailed description of the close vicinity of the specific polyion (DNA molecule) while our method provides global features of charge distribution around the polyion. One can perceive some combination of both methods with division of space into three regions with different levels of description: water molecules plus ions; ions in the effective dielectric media; continuous charge distribution.

The results presented here indicate that the unification of self consistent field and MC methods yields a good facility for calculations of equilibrium ionic densities and potential with optimal use of computer time. In its final formulation (Section 3) the MC–SCF method can be easily applied to models with the specific structure of the polyion: in the internal region the standard MC procedure would readily account for all the inhomogeneities; for distances $r > R_M$ the inhomogeneities are already smoothed to a considerable degree.

APPENDIX 1

Evald Method for Cylindrical Polyion

For a complete description of the infinite cylinder in MC simulations one should use periodic boundary conditions: a cylindrical MC cell of the height h is periodically translated along the axis Z of the polyion. To account for interactions with ions outside the basic cell it is necessary to calculate the sum:

$$V(r, r_0) = \sum_{j=-\infty}^{\infty} \frac{1}{|r - r_j|}, \tag{A1}$$

where $r_j = r_0 + jhe_z$, and e_z is the unit vector along z axis, r is the position of an ion in the basic cell, and r_j are the positions of another ion in the basic cell ($j = 0$) and of its images in other cells. In order to calculate this sum in MC procedure practically Evald method [32] can be applied. Start with the following identify:

$$\frac{1}{|r - r_j|} = \frac{2}{\pi} \int_0^{\infty} d\rho \exp(-\rho^2 |r_j - r|^2).$$

One can present this integral as a sum of two parts: from 0 to D (let it be V_1) and from D to ∞ (V_2) and calculate them separately.

$$V_2 = \sum_{j=-\infty}^{\infty} \frac{2}{\pi} \int_D^{\infty} d\rho \exp(-\rho^2 |r - r_j|^2) = \sum_{j=-\infty}^{\infty} \frac{\operatorname{Erfc}(D|r - r_j|)}{|r - r_j|}. \tag{A2}$$

Presenting another part we use notations $r^{\parallel}$ and $r^{\perp}$ projections of vector r onto the Z axis and onto the normal plane. V_1 is a periodic function and it can be expressed as a Fourier series:

$$V_1 = \sum_{j=-\infty}^{\infty} \frac{2}{\pi} \int_0^{D} d\rho \exp(-\rho^2 |r - r_j|^2) = \frac{2}{\pi} \int_0^{D} d\rho \sum_{k=-\infty}^{\infty} c_k \exp \frac{2\pi i k r''}{h}, \tag{A3}$$

where

$$\begin{aligned} c_k &= \frac{1}{h} \int_{-h/2}^{h/2} dr'' \sum_{j=-\infty}^{\infty} \exp(-\rho^2 |r_j^{\perp} - r^{\perp}|^2) \exp(-\rho^2 |r_j'' - r''|^2) \exp \frac{-2\pi i k r''}{h} \\ &= \frac{1}{h} \exp(-\rho^2 |r_0^{\perp} - r^{\perp}|^2) \int_{-\infty}^{\infty} dr'' \exp[-\rho^2 (r_0'' - r'')^2] \exp \frac{-2\pi i k r''}{h} \\ &= \frac{\pi}{2h} \exp(-\rho^2 |r_0^{\perp} - r^{\perp}|^2) \frac{1}{\rho} \exp\left(-\frac{\pi^2 k^2}{\rho^2 h^2}\right). \end{aligned} \tag{A4}$$

Substituting Equation (A4) into Equation (A3) after some transformations we obtain:

$$\begin{aligned} V_1 = {} & \frac{1}{h} \int_0^{D} \frac{d\rho}{\rho} \exp(-\rho^2 |r_0^{\perp} - r^{\perp}|^2) + \frac{2}{h} \sum_{k=1}^{\infty} \int_0^{D} \frac{d\rho}{\rho} \\ & \times \cos \frac{2\pi k (r'' - r_0'')}{h} \exp\left(-\rho^2 |r_0^{\perp} - r^{\perp}|^2 - \frac{\pi^2 k^2}{\rho^2 h^2}\right). \end{aligned}$$

The integral in the first term diverges at zero (since the initial sum (A1) diverges).

The infinite constant can be subtracted thus yielding to:

$$V(r, r_0) = \sum_{j=-\infty}^{\infty} \frac{\mathrm{Erfc}\,(D|r - r_j|)}{|r - r_j|} - \frac{1}{h}\int_0^D \frac{\mathrm{d}\rho}{\rho}\,[1 - \exp(-\rho^2|r^\perp - r_0^\perp|^2)]$$
$$+ \frac{2}{h}\sum_{k=-\infty}^{\infty}\int_0^D \frac{\mathrm{d}\rho}{\rho}\cos\frac{2\pi k(r_0'' - r'')}{h}\exp\left(-\rho^2|r^\perp - r_0^\perp|^2 - \frac{\pi^2k^2}{\rho^2h^2}\right) + \text{const.}, \tag{A5}$$

where

$$\text{const.} = \frac{1}{h}\int_0^D \frac{\mathrm{d}\rho}{\rho}.$$

Expression (A5) consists of two quickly converging series and by an appropriate choice of D it is possible to achieve equal rate of convergence for both series. For $D = 1/h$ we get the ultimate result:

$$V(r, r_0) = \sum_{j=-\infty}^{\infty} \frac{\mathrm{Erfc}(|r - r_j|)/h}{|r - r_j|}\frac{1}{h}\int_0^{1/h} \frac{\mathrm{d}\rho}{\rho}\,[1 - \exp(-\rho^2|r^\perp - r_0^\perp|^2)]$$
$$+ \frac{2}{h}\sum_{k=-\infty}^{\infty}\int_0^{1/h} \frac{\mathrm{d}\rho}{\rho}\cos\frac{2\pi k(r_0'' - r'')}{h}\exp\left(-\rho^2|r^\perp - r_0^\perp|^2 - \frac{\pi^2k^2}{\rho^2h^2}\right) + \text{const.} \tag{A6}$$

Expression (A6) depends on two parameters: $(r'' - r_0'')$ and $|r^\perp - r_0^\perp|$. The corresponding two-dimensional table is calculated and stored in the memory before simulation.

In ordinary NVT-ensemble MC simulations the constant in Equation (A6) is of no importance since in difference of energies it is canceled. However in transitions with the change in the number of particles it is necessary to make concordant calculations of the energy change for the internal and external regions. To achieve this consistency a certain constant should be added to the Evald potential (A6) providing fulfilling of the following asymptotic condition:

$$V(r'', r^\perp) \underset{r^\perp \to \infty}{\sim} (2/h)\ln(r^\perp). \tag{A7}$$

This condition corresponds to the fact that the potential calculated by Evald method for a linear chain of point charges should coincide at great distances with the potential of a uniformly charged infinite straight line with the corresponding linear charge density.

References

[1] G.S. Manning, "The Molecular Theory of Polyelectrolyte Solutions with Application to the Electrostatic Properties of Polynucleotides", *Quart. Rev. Biophys.*, **11**, 179 (1978).

[2] M. Fixman, "The Poisson–Boltzmann Equation and its Application to Polyelestrolytes", *J. Chem. Phys.*, **70**, 4995 (1979).

[3] C.L. Steven and T.M. Glenn, "The Statistical Mechanics of the Electrical Double Layer", *Adv. Chem. Phys.*, **56**, 141 (1984).

[4] M.D. Frank-Kamenetskii, V.V. Anshelevich and A.V. Lukashin, "Polyelectrolyte Model of DNA", *Sov. Phys. Uspekhi*, **30**, 317 (1987).

[5] E.G. Tovar, H. Losada-Cassou and D. Henderson, "Hypernetted Chain Approach for the Distribution of Ions around a Cylindrical Electrode. II. Numerical Solution for a Model Cylindrical Polyelectrolyte", *J. Chem. Phys.*, **83**, 361 (1985).

[6] G.V. Ramanathan, "Statistical Mechanics of Electrolytes and Polyelectrolytes. III. The Cylindrical Poisson–Boltzmann Equation", *J. Chem. Phys.*, **78,** 3223 (1983).
[7] R. Bacquet and P.J. Rossky, "Ionic Atmosphere of Rod-like Polyelectrolytes. A Hypernetted Chain Study", *J. Phys. Chem.*, **88,** 2660 (1984).
[8] L. Belloni, "A Hypernetted Chain Study of Highly Assymetrical Polyelectrolytes", *Chem. Phys.*, **99,** 43 (1985).
[9] H. Wennerstrom and B. Lindman, "Micelles. Physical Chemistry of Surfactant Association", *Phys. Rep.*, **52,** 1 (1979).
[10] B. Jayaram and D.L. Beveridge, "Grand Canonical Monte Carlo Simulations on Aqueous Solutions of NaCl and NaDNA: Excess Chemical Potential and Sources of Nonideality in Electrolyte and Polyelectrolyte Solutions", *J. Phys. Chem.*, **95,** 2506 (1991).
[11] V. Vlachy and A.D.J. Haymet, "A grand canonical Monte Carlo Simulation Study of Polyelectrolyte Solutions", *J. Chem. Phys.*, **84,** 5874 (1986).
[12] C.S. Murthy, R.J. Bacquet and P.J. Rossky, "Ionic Distribution near Polyelectrolytes. A Comparison of Theoretical Approaches", *J. Phys. Chem.*, **89,** 701 (1985).
[13] C.W. Outhwaite, "A Modified Poisson–Boltzmann Equation for the Ionic Atmosphere around a Cylindrical Wall", *J. Chem. Soc., Faraday Trans. 2*, **82,** 789 (1986).
[14] P.N. Vorontsov-Velyaminov and A.P. Lyubartsev, "Combining of the Monte Carlo and Self Consistent Field Methods in the Theory of DNA and other Polyelectrolytes", *Vestnik LGU (Leningrad)* **4,** 13 (1987).
[15] P.N. Vorontsov-Velyaminov and A.P. Lyubartsev, "Self-Consistent Field – Monte Carlo Method in the Polyelectrolyte Theory. Calculation of the Electrostatic Potential for the Symmetrical Polyions", *Molek. Biol. (Moscow)*, **21,** 654 (1987).
[16] P.N. Vorontsov-Velyaminov and A.P. Lyubartsev, "Monte Carlo – Self Consistent Method in the Polyelectrolyte Theory," *J. Biomol. Struct. and Dyn.*, **7,** 739 (1989).
[17] A.P. Lyubartsev, V.P. Kurmi and P.N. Vorontsov-Velyaminov, "Monte Carlo – Self Consistent Field Simulation of the Interaction of Single- and Divalent Ions with DNA", *Molek. Biol. (Moscow)*, **24,** 1533 (1990).
[18] B.J. Klein and G.R. Pack, "Calculation of the Spatial Distribution of the Charge Density in DNA Environment", *Biopolymers*, **22,** 2331 (1983).
[19] J. Conrad, M. Troll and B.H. Zimm, "Ions Distribution with Improved Electrostatic Potential", *Biopolymers*, **27,** 1361 (1988).
[20] J.P. Valleau and L.K. Cohen, "Prititive Model of Electrolytes. I. Grand Canonical Monte Carlo Computations", *J. Chem. Phys.*, **72,** 5935 (1980).
[21] G.M. Torrie and J.P. Valleau, "Electrical Double Layer. I. Monte Carlo Study of a Uniformly Charged Surface", *J. Chem. Phys.*, **73,** 5807 (1980).
[22] B. Widom, "Some Topics in the Theory of Liquids", *J. Chem. Phys.*, **39,** 2808 (1963).
[23] S.V. Slonitski, E.V. Frisman, A.K. Valeev and A.M. Elyashevich, "Intrinsic Viscosity Calculation of the Synthetic and Biological Polyelectrolytes of Various Rigidity", *Molek. Biol. (Moscow)*, **14,** 484 (1980).
[24] A.P. Lyubartsev and P.N. Vorontsov-Velyaminov, "Monte Carlo Simulations of Flexible Polyelectrolytes", *Macromolecular Compounds (Moscow)*, **32,** 721 (1990).
[25] Z. Alaxandrowicz, "Effect of Excluded Volume on Polyelectrolytes in Salt Solutions", *J. Chem. Phys.*, **11,** 4377 (1967).
[26] P.M. Davis and W.B. Russel, "On the Theory of Dilute Polyelectrolyte Solutions: Extension, Refinements and Experimental Tests", *J. Polym. Sci. B*, **24,** 511 (1986).
[27] M. Fixman, "Radius of Gyration of Polymer Chains. II. Segment Density and Excluded Volume Effects", *J. Chem. Phys.*, **36,** 3123 (1962).
[28] M.A. Sibileva, A.N. Veselkov, S.V. Shilov and E.V. Frisman, "Effect of the Temperature on Conformation of the Native DNA Molecule in Aqueous Solution of Different Electrolytes", *Molek. Biol. (Moscow)*, **21,** 140 (1987).
[29] A.Z. Panagiotopoulos, "Direct Determination of Phase Coexistence Properties of Fluids by Monte Carlo Simulations in New Ensemble", *Molec. Phys.*, **61,** 813 (1987).
[30] D.M. Tsangaris and P.D. McMahon, "A Modified Gibbs Ensemble Method for Calculating Fluid Phase Equilibria", *Molecular Simulation*, **7,** 97 (1991).
[31] E. Clementi, "Structure of Water and Counterions for Nucleic Acids in Solution", *Struct. and Dyn. Nucl. Acids and Proteins*, New York, Adenine Press, p. 321 (1983).
[32] C. Kittel, *Introduction to Solid State Physics*, Wiley, New York, 1986, Appendix B.